ELSEVIER

Journal of Photochemistry and Photobiology A: Chemistry 112 (1998) 261–270

Journal of Photochemistry and Photobiology A:Chemistry

Photocatalytic oxidation of 2,4-dichlorophenoxyacetic acid with titania photocatalyst. Comparison of supported and suspended TiO_2

A.D. Modestov [1], O. Lev *

Division of Environmental Sciences, The Fredy and Nadine Herrmann School of Applied Science, The Hebrew University of Jerusalem, Jerusalem, 91904, Israel

Received 18 August 1997; accepted 15 September 1997

Abstract

The photodegradation of 2,4-dichlorophenoxyacetic acid using illuminated titania particles was studied in buffered water solutions at pH 9.2. A simplified phenomenological model which enables comparison of activity of suspended and supported photocatalyst on the basis of utilisation of light is proposed. The model shows saturation of photodegradation rate with increase of amount of photocatalyst on support or in suspension. The features of the model were verified by studies of the photocatalytic activity of TiO_2 suspended and supported on flat glass plate and on floating particles.

Keywords: Photodegradation; 2,4-D; Titania; Photocatalysis

1. Introduction

Illuminated TiO_2 is a powerful oxidiser due to the formation of holes in the valence band by photoexcitation. The level of the TiO_2 valence band is approximately 3 V below the hydrogen equilibrium, which makes it possible to oxidise nearly any organic impurity in water. Halogenated hydrocarbons are among most widely spread toxic impurities in water. They are used in agriculture as pesticides; they are readily formed in oxidative disinfection processes; and they are ubiquitous in industrial wastes. It was shown that haloaromatic compounds, such as 2,4,5-trichlorophenoxyacetic acid and 2,4,5-trichlorophenol, as well as chlorinated hydrocarbons, can be decomposed and even mineralised by illuminated titania [1–6].

For water purification, TiO_2 photocatalyst can be used as a suspension or on a support. In the latter case, it is used as a coating on illuminated buoyant glass beads [7,8], glass fibre cloth [9], and walls of the vessels of various shapes [10,11], including tube and falling film photoreactors. A common basis for comparison of the activity of supported and suspended TiO_2 is required. Generally, activity of different catalysts is compared by relating the oxidation rate per unit weight of the active photocatalyst. Degussa P-25 TiO_2 is often used as a standard for comparison. However, such approaches cannot straightforwardly be used for comparing different forms of catalysts, such as suspended and supported TiO_2. For systems based on artificial light sources, electric power expenses for light generation are substantially higher than the price of the catalyst [11]. Similarly, for solar systems reactor area considerations are more important than the titania costs. This implies that comparison of catalysts can be done on the basis of utilisation of light, rather than on TiO_2 loading. Though there are advanced theoretical treatments on the activity of single nanometer size titania particle in the photocatalytic systems [12–14], the tool for evaluation of the activity of ensemble of particles in suspension or supported titania films in terms of light efficiency still have to be developed. The main obstacle in this field, in our opinion, is the elaboration of light intensity distribution function inside the reactor. Though, the evaluation of light distribution function in systems involving light scattering is rather complex [15–18], there were several attempts to take into account light scattering in reactor design [19].

In the present work an attempt is made to elaborate a simple phenomenological approach for studies of photocatalytical activity of suspended and supported photocatalysts on the basis of light utilisation. Light scattering by the photocatalyst particles is neglected. The supported catalyst composed of nanoparticles and aggregates of nanoparticles is treated as a

---

* Corresponding author.

[1] On leave from A.N. Frumkin Institute of Electrochemistry, Russian Academy of Sciences, Russia.

1010-6030/98/$19.00
PII S1010-6030(97)00269-4

porous, but optically homogeneous body. Particles of titania are characterised by light absorption coefficient α or by photon capture cross-section σ. All particles on support or in suspension are considered to be easily accessible by target compound dissolved in solution, i.e., internal and external diffusion limitations are assumed to be negligible. On this basis, the dependence of photocatalytic oxidation rate on thickness of supported titania layer is compared to the dependence of photocatalytic activity of suspended titania on its concentration.

The theoretical approach was supported by activity evaluation of titania using the photocatalytical oxidation of 2,4-dichlorophenoxyacetic acid (2,4-D), a widely used herbicide. Dependence of the photocatalytic activity of titania on its concentration was measured with titania P-25 produced by Degussa and titania supplied by Aldrich. Size of aggregates formed in suspensions was determined and compared with parameters of the photocatalytic process. The activity of titania P-25 supported on flat glass and on buoyant particles was determined and compared to the activity of suspended titania.

2. Experimental details

Photocatalytic experiments were carried out by irradiation of open cylindrical vials, containing 50–100 ml of aerated and stirred, buffered aqueous solution of 2,4-D and appropriate amount of photocatalyst. Irradiation was carried out with 300 W Oriel ozone free Xe lamp. The lamp was equipped with a dichroic mirror producing light beam of 280–400 nm wavelength band. An additional glass filter absorbed the light of wavelength shorter than 300 nm. Unless otherwise stated, intensity of light hitting the surface of solution was adjusted to 60 $mW^* cm^{-2}$ by a light intensity monitor (Ophir thermopile, Nova). The vial containing the test solution was maintained at constant temperature by a water jacket and a thermostat. Experiments were conducted at constant temperature, 25°C. Blank experiments, without photocatalyst, were carried out to ensure lack of direct photolysis of the target compound. Concentration changes of 2,4-D were determined by monitoring the 2,4-D light absorption peak at 283 nm by a Varian Cary 1E UV–vis spectrophotometer. For analysis of total organic carbon (TOC) and concentration of Cl^- ions the irradiation experiments were terminated after appropriate time intervals and the sample was taken for analysis. So, each data point represents a separate experiment. TOC measurements were performed using Dohrmann DC-80 automated laboratory total organic carbon analyser. Initial solution was used as a standard. Concentration of Cl^- was determined by titration of acidified solution by 0.01 N $AgNO_3$, using Metrohm 673 Titroprocessor combined with a silver electrode No 6.0404.100. Particle size distribution in suspension was determined by a Malvern Autoisizer 2c, (UK), based on scattering of 632 nm He–Ne laser beam. Diffuse reflectance spectroscopy measurements of supported TiO_2 were performed using Varian Cary 1E spectrophotometer equipped with a diffuse reflectance accessory.

2,4-dichlorophenoxyacetic acid was supplied by Applied Science Lab. Titania P-25 Degussa was donated by Degussa. Point of zero charge of titania P-25 suspension was reported to be at pH 6.3 [20]. At higher pH values titania particles are negatively charged. Solutions were buffered at pH 9.2 using 0.01 N $Na_2B_4O_7$ to ensure low adsorption of 2,4-D anions by the negatively charged titania particles. TiO_2 suspensions were prepared by sonication for 5 min. Sample solutions containing TiO_2 suspension were centrifuged before analysis to minimise turbidity interference. TiO_2 P-25 consists of primary particles of 30 nm average diameter [21,22]. Aldrich titania particles were characterised by a broad distribution of particle size in the range 10–50 nm. Primary particles of titania form aggregates of diameter approximately 0.3–0.5 micrometer [21].

TiO_2 coating on glass plates was performed by repeated sol–gel dip-coating on glass plates, which were degreased in methanol. Organically modified silica (Ormosil) was used as hydrophobic binder. Coating solution contained 20 ml of methanol, 0.2 g of TiO_2 P-25, and appropriate amount of methyltrimethoxysilane (MTMOS), which was set to achieve the desired TiO_2/Ormosil weight ratio. 3-fold excess of water for hydrolysis of MTMOS was added as 1 N HCl. Solutions were allowed to hydrolyse for 3 h before coating was performed.

The buoyant particles coated with titania P-25 were prepared by coating exfoliated graphite (EG) particles in methanol solution containing MTMOS and titania P-25 suspension, as described elsewhere [23]. Exfoliated graphite was purchased from NIIGRAFIT, Moscow (Russia). It is characterised by a bulk density of approximately 20 $g^* l^{-1}$, BET surface area of 20 $m^{2*} g^{-1}$ and 10–15% closed pores by volume. Particles were irregular by shape, mostly in the form of twisted cylinders. The average size of the particles was ca. 0.5 mm. The overall composition of particles of photocatalyst was EG:Ormosil:titania = 1:1:1 (by weight). 1 g of floating particles covered approximately 60 cm^2 of water surface.

3. Theoretical approach

The photocatalytic oxidation of organic species on titania photocatalyst is a complicated process, which depends on the concentration of reacting species, namely: the organic species and dissolved oxygen in solution, amount of titania and its activity, and the light flux distribution in the reaction vessel. The following description of the processes occurring at a single illuminated TiO_2 particle is based on the scheme given by Gerischer and Heller [12] and Gerischer [13,14].

Firstly, we shall consider photodegradation by a layer of photocatalyst on a flat support in water solution containing the reactants: oxygen and target organic compound. A layer of thickness, h, of titania nanoparticles is placed on a flat horizontal surface of area, S, in a vial illuminated from the top parallel to the z-axis. Axes x, y are in layer plane. The light propagation inside the porous layer is treated as a propagation in a uniform layer. This means that scattering of light by the nanometer scale pores is neglected. Light is assumed to be monochromatic with wavelength λ. Light beam irradiates the sample with uniform light intensity I_0. The pores occupy $(1-\theta) \ll 1$ fraction of the layer volume. We assume that the porous layer is fully wetted by the solution and all particles are equally accessible by the target compounds. Illumination of titania particle results in the formation of photoexcited electrons in conduction band and holes in the valence band. Photoexcited charge carriers reaching the particle surface react with the appropriate species in solution. Surface reaction of holes with target compound AH_2 with rate constant starts the oxidation chain:

$$AH_2+[p_s]\rightarrow AH^*+H^+. \tag{1}$$

Photoexcited electrons are scavenged by dissolved oxygen. Absorption of light by a spherical nanometer size TiO_2 particle of diameter d, surface area $s=\pi d^2$ and volume $v=(1/6)\ \pi d^3$ is equal to [13]:

$$\begin{aligned}&(1-R)(0.25\pi d^2)I[1-\exp(-\alpha\gamma d)]\\&\quad\cong 0.25\gamma(1-R)\pi d^3\alpha I,\end{aligned} \tag{2}$$

where α is the light absorption coefficient of titania for the irradiation wavelength, $\gamma<1$ is a correction factor for particle shape, and the term $(1-R)$ accounts for all reflections by the photocatalytic particle. In further treatments reflection of light is neglected, i.e., $R=0$. Recombination of excited electron-hole pairs is often a dominant consumption path of photoexcited holes. Thus, under such conditions the surface concentration of holes is proportional to the square root of light intensity, see Eq. (18b) in [13]:

$$[p_s]=k\sqrt{(\alpha I)} \tag{3}$$

The oxidation rate of AH_2 at a single illuminated TiO_2 particle in solution is given by:

$$r=k_{ox}[AH_2]_s[p_s]s=k_{ox}[AH_2]_s sk\sqrt{(\alpha I)}, \tag{4}$$

where k_{ox} is the heterogeneous oxidation rate constant. Taking into account, that number of particles per unit of volume of layer is θ/v, the total reaction rate, w can be determined by integrating Eq. (4) over layer volume hS. Assuming, that concentration of AH_2 at the particle surface is equal to the volume concentration of dissolved AH_2 (i.e., $[AH_2]_s=[AH_2]$), then the change of concentration of AH_2 inside the vessel volume V with irradiation time t, is given by:

$$\begin{aligned}&V\mathrm{d}[AH_2]/\mathrm{d}t=w\\&\quad=(k_{ox}[AH_2]ks(\theta/v)\sqrt{\alpha}\int_0^V\!\!\int\!\!\int\sqrt{I}\,\mathrm{d}x\,\mathrm{d}y\,\mathrm{d}z\\&\quad=K[AH_2]S\theta\sqrt{\alpha}\int_0^h\sqrt{I}\,\mathrm{d}z\end{aligned} \tag{5}$$

where $K=k_{ox}k(s/v)$. Since the light intensity I is assumed to be independent of x, y, the integration over these coordinates is simply given by multiplication of the integrand by S, the vial cross-section area.

The quantity K contains the main photocatalytic parameters of the primary titania particle, which are independent of whether it is in suspension or on support. Due to light absorption in the porous TiO_2 layer, the light intensity changes with the depth z as:

$$I=I_0\exp(-\alpha\theta z), \tag{6}$$

where I_0 is the light intensity hitting the top of the titania layer. Integration of Eq. (5) over the thickness of the TiO_2 layer using the light intensity distribution of Eq. (6) gives:

$$V\mathrm{d}\{\ln[AH_2]\}/\mathrm{d}t=2KS\sqrt{(I_0/\alpha)}\{1-\exp(-0.5\alpha\theta h)\} \tag{7}$$

Eq. (7) indicates, that the photocatalytic activity reaches saturation as the layer thickness increased. The slope of dependence of $\ln[AH_2]$ on irradiation time t, measured at $0.5\ \alpha\theta h \ll 1$, using the approximation $\{1-\exp(-0.5\ \alpha\theta h)\} \approx 0.5\ \alpha\theta h$, can be used for determination of the value of the product $\theta/\sqrt{\alpha}$

The photocatalytic activity of suspension of photocatalyst can be derived by the same way. Assuming, that the titania aggregates are cubic of uniform size, and small enough not to cast shade on neighbouring aggregates due to diffraction of light [24] ($D\leq\lambda$, $D\ll L$ where L is average distance between neighbouring aggregates, D is the aggregate size, and λ is the irradiation wavelength), one can obtain the light intensity distribution function over a vial filled with suspended titania. For simplicity, each aggregate can be treated as a separate cubic section of titania layer of thickness D and cross-section area D^2. Thus, the activity of a single aggregate can be described using the equations derived for titania layer, Eqs. (5)–(7). The aggregate can be characterised by photon capture cross-section σ. Decay of light intensity $\mathrm{d}I$ in a solution layer of thickness $\mathrm{d}z$ is proportional to the concentration of aggregates n:

$$-\mathrm{d}I=In\sigma\,\mathrm{d}z \tag{8}$$

Integration of Eq. (8) over the vial depth gives:

$$I=I_0\exp(-n\sigma z) \tag{9}$$

The photon capture cross-section can be taken as:

$$\sigma=D^2(1-\exp(-\alpha\theta D)) \tag{10}$$

where D^2 is the cross-section area of aggregate, θ is the fraction of aggregate volume occupied by titania, and the term in brackets takes into account the penetration of light through aggregate. According to Eq. (7), each aggregate destroys AH_2 with the rate of:

$$w=2KD^2[AH_2]\sqrt{(I/\alpha)}\{1-\exp(-0.5\alpha\theta D)\} \qquad (11)$$

where D^2 is the cross-section area of aggregate and I is the light intensity hitting the aggregate. Integration of Eq. (11) over a vial, characterised by cross-section area S, solution height H, and volume $V=SH$, with light intensity distribution function of Eq. (9) and photon capture cross-section of Eq. (10) gives:

$$V\,d\{\ln[AH_2]\}/dt=4KS\sqrt{(I_0/\alpha)}$$
$$\times\{1-\exp(-0.5nD^2(1-\exp(-\alpha\theta D))H)\} \qquad (12)$$

The general form of Eq. (12) indicates, that the process of photodegradation by suspension of particles can be represented as pseudo-heterogeneous chemical process characterised by pseudo-reaction surface–cross-section area of the illuminated vial, S and pseudo-heterogeneous reaction rate constant K_{ps}, with photon flux I_0 participating as a reactant:

$$V\,d\{\ln[AH_2]\}/dt=\boldsymbol{K}_{ps}S\sqrt{I_0} \qquad (13)$$

The pseudo-heterogeneous rate constant, K_{ps} depends on the amount and optical properties of light absorbing particles, as well as on parameters characterising the chemical processes. It is worth mentioning, that for low value of $(n\sigma H)\ll 1$, K depends linearly on the amount of photocatalyst, n, but it reaches saturation at high values of $(n\sigma H)$. Two limiting forms of Eq. (12) can be considered.

The first case arises, when suspension is composed only of nanoparticles of TiO_2, ($\theta=1$) or small aggregates, with the particle size much smaller than light penetration depth ($0.5\ \alpha d\ll 1$). In this case Eq. (12) transforms into:

$$V\,d\{\ln[AH_2]\}/dt=4KS\sqrt{(I_0/\alpha)}$$
$$\times\{1-\exp(-0.5nd^3\alpha\theta H)\} \qquad (14)$$

In a second limiting case, formation of aggregates of large size ($0.5\ \alpha D\gg 1$) is envisaged. Light does not penetrate through aggregate. In this case Eq. (12) is transformed into:

$$V\,d\{\ln[AH_2]\}/dt=4KS\sqrt{(I_0/\alpha)}$$
$$\times\{1-\exp(-0.5nD^2H)\} \qquad (15)$$

It is worth mentioning, that because of the strong dependence of light absorption coefficient on the photoexcitation wavelength, the reaction rate can follow Eq. (14) for long wavelength irradiation and Eq. (15) at irradiation at shorter wavelengths.

The structures of Eq. (7), Eqs. (14) and (15) are quite similar. In all cases degradation rate follows the light absorption by photocatalyst: the degradation rate increases with the increase of amount of TiO_2 at low loading, and reaches saturation at high loading, when practically all light is absorbed.

It is important, that the pseudo-heterogeneous rate constant of photodegradation does not depend explicitly on the total surface of photocatalyst particles (Eq. (7), Eqs. (14) and (15)). Eqs. (14) and (15) indicate, that amount of TiO_2 particles in suspension influence the degradation rate as a function of the product of solution height and TiO_2 concentration, which is proportional to titania loading per unit of illuminated area. It indicates, that comparison of degradation rate observed with photocatalysts of different forms (suspended and supported) can be based on TiO_2 loading per unit of illuminated surface area, for both, suspended and supported, photocatalysts. Expressions (14) and (15) indicate that saturation value of degradation rate with suspension at a given light intensity is independent of aggregation of primary particles. Another important feature of comparison of Eq. (7), Eqs. (14) and (15) at high TiO_2 loading is the exactly twice higher degradation rate with suspended photocatalyst compared to the degradation with supported TiO_2 film of the same apparent area S, though the suspension was treataed as a fractured layer. This paradox is caused by the nonlinear dependence of oxidation rate on light intensity (Eqs. (3) and (4)), and it vanishes, when surface concentration of holes is proportional to the light intensity. For square root dependence, the higher the light intensity, the lower is the efficiency of light utilization by photocatalyst. To attain the highest efficiency of light utilization the given amount of photons should be spread over the largest possible area of TiO_2, so that each particle of TiO_2 works at the lowest possible light intensity. In the case of suspension, where particles are far enough from each other to enable redistribution and averaging by light diffraction, the effective light intensity is smaller than in the case of a densely packed layer. The following simple model can illustrate this effect. A cylinder of cross-section area S is filled with solution of target compound. Multiple horizontal layers of photocatalyst on flat support are located perpendicular to the incident light beam. Each layer consists of micrometer size squares of photocatalyst covering 0.5 S. In each layer photocatalyst sites and holes are located in a chess like manner. Each brick of the photocatalyst is thick enough to absorb all light falling on it. The layers are distant enough to make illumination of each layer homogeneous by light diffraction. The degradation rate, ascribed to uniform layer of photocatalyst of area S illuminated with total light flux, F, is W. In our model, the upper layer, which is characterised by an apparent area 0.5 S, absorbs half of the total light flux F, and destroys AH_2 with rate 0.5 W. A second layer, illuminated with homogeneous light flux 0.5 F absorbs half of it and degrades AH_2 with a rate of $0.5\sqrt{0.5}\ W=0.354\ W$. Accordingly, the third, fourth, fifth and sixth layers destroy AH_2 with degradation rates of 0.25 W, 0.177 W, 0.125 W, and 0.088 W, respectively. Summing up degradation rate over infinite number of layers gives 1.707 W. If each layer absorbs only small fraction of light flux, γF ($\gamma\rightarrow 0$), the sum over infinite number of layers gives 2 W. On the other hand, if layers are close enough to cast a shadow onto the layer located below, the photocatalyst squares are illuminated at full light intensity or they are located in shadows. In this case, the sum efficiency is equal to 1 W.

The square root and linear dependencies of photodegradation rate with photocatalysts on light flux are extreme cases of dependence of surface concentration of holes on irradiation intensity [12–14]. For intermediate cases one can expect that the difference between the rates observed with suspended and supported photocatalyst of infinite loading of photocatalyst would be between 1 and 2, assuming absence of diffusion limitations.

4. Results and discussion

Fig. 1 presents concentration changes during the photocatalytic oxidation of 2,4-D by P-25 suspension. The photocatalytic oxidation is a multistage process. The decay of UV absorption peak indicates the disappearance of the initial compound. This process, under conditions of Fig. 1, is characterised by a half-life period of approximately 20 min. The half time period of Cl^- release is approximately 110 min. The half-life period measured for TOC removal is approximately 13 h, which is about 40 times longer than the half life of 2,4-D. Taking into account, that for full mineralization of a 2,4-D molecule 32 holes are required, while one hole is sufficient for elimination of a 2,4-D molecule, one can conclude that the first step in photodegradation of 2,4-D proceeds at the average rate of the degradation of the 2,4-D oxidation by-products (i.e., TOC removal). A mechanism for the photodegradation of 2,4-D by illuminated TiO_2, at pH 4 was proposed by Pichat et al. [25]. The initial reaction of photodegradation of 2,4-D at pH $\cong$ 4 is the decarboxylation:

$$\text{R-OCH}_2\text{-COO}^- + p^+ \rightarrow \text{R-OCH}_2^* + \text{CO}_2 \qquad (16)$$

However, in our experiments, which were conducted at pH 9.2, the TOC of the solution was almost constant during the first 100 min of illumination. It implies that Eq. (16) is not the dominant reaction in the initial stage of 2,4-D degradation. The hydroxylation and chloride removal reactions, which are not accompanied by TOC reduction, are, probably, competing reactions.

Fig. 2 shows changes of the concentration of 2,4-D monitored by reduction of the UV absorption peak during irradiation of solutions containing P-25 and Aldrich TiO_2. The slope of degradation curve was used for the determination of the pseudoheterogeneous degradation rate constant at a given light intensity:

$$K^1_{ps} = (V/S)\ \mathrm{d}(\ln C)/\mathrm{d}t \qquad (17)$$

where, V and S are the solution volume and vial cross-section area respectively, C stands for concentration of 2,4-D in solution. The square root of light intensity, which was kept constant and light absorption coefficient, α are included in a combined rate constant $K_{ps}{}^1$.

Fig. 3 shows the dependence of diffuse reflectance of titania coated (P-25:Ormosil = 6) glass slide on the light wavelength. The overall loading was 1.1 mg cm^{-2}. The diffuse reflectance coefficient falls sharply with the onset of fundamental absorption from a value of 95% at $\lambda = 410$ to 4% at $\lambda = 300$ nm. The low value of light reflection coefficient (17%) at $\lambda = 350$ nm confirm, that light scattering by TiO_2 particle can be neglected in our experimental conditions.

Fig. 4 shows the dependence of 2,4-D pseudo-heterogeneous degradation rate constant on loading of P-25 or Aldrich TiO_2 in suspension. The $K_{ps}{}^1$ was determined according to Eq. (17). The dependence reaches saturation in agreement with Eq. (12). The saturation value of $K_{ps}{}^1$ for P-25 is 2.5 times larger than for Aldrich TiO_2. Similar difference in activity of P-25 and Aldrich TiO_2 was observed by others, as well [26]. The saturation of degradation rate with increase of TiO_2 concentration was observed by many researchers, e.g., [27,28], however detailed comparison of curves is not pos-

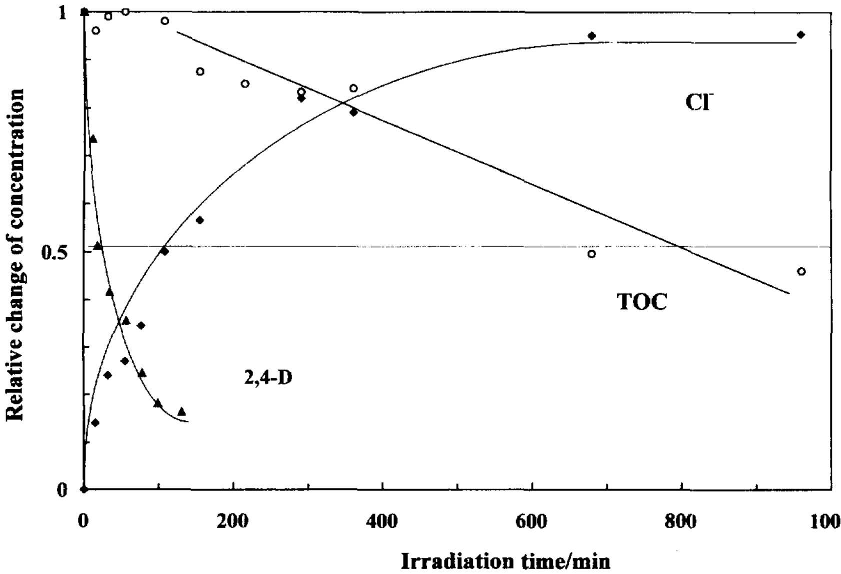

Fig. 1. Relative changes of concentration of 2,4-D, Cl^- ions and TOC during irradiation of 100 ml of 50 ppm 2,4-D in presence of 4 mg P-25 suspension. Irradiation intensity 60 mW* cm^{-2}, vial cross-section area 18 cm^2.

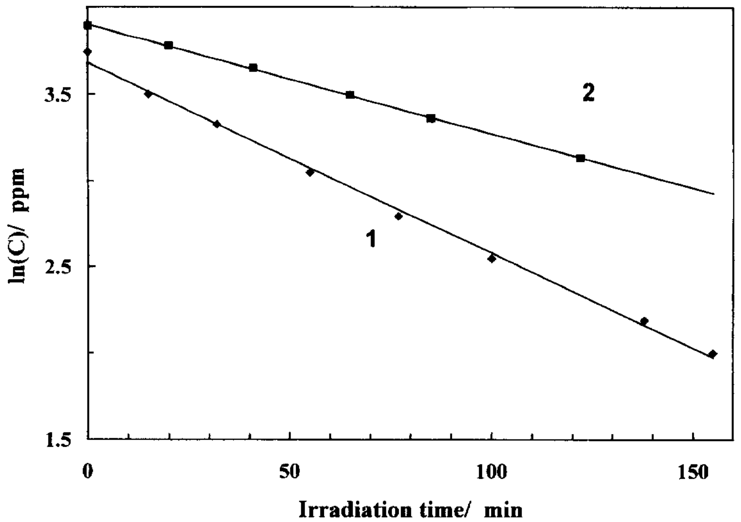

Fig. 2. Dependence of logarithm of concentration of 2,4-D on time of irradiation with light intensity 60 mW* cm^{-2} in presence of 4 mg TiO_2 suspensions, vial cross-section area 18 cm^2. Curve '1'-P-25 TiO_2, solution volume 100 ml; curve '2'. Aldrich TiO_2, solution volume 60 ml.

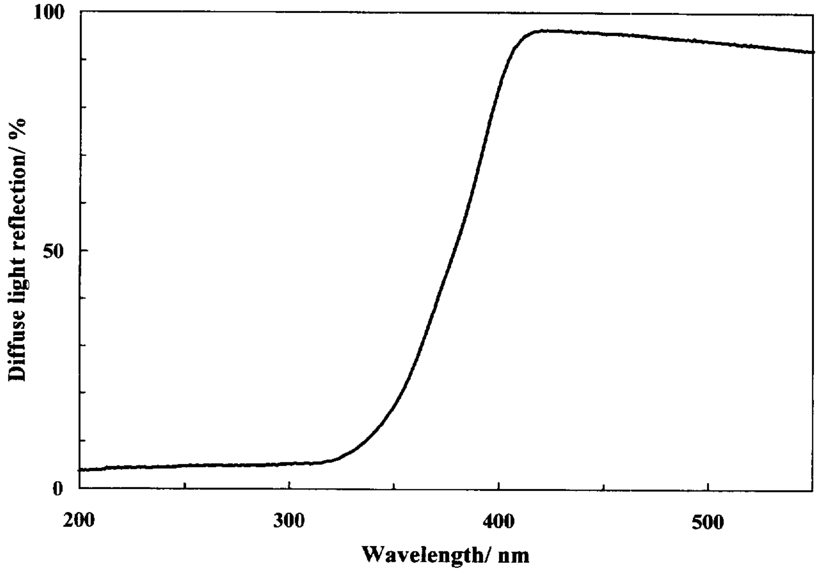

Fig. 3. Diffuse reflectivity-light wavelength dependence of titania coated glass slide (composition P-25:Ormosil = 6).

sible, as solution height was not reported. The decrease of quantum yield with increase of light excitation wavelength was observed by Valladares and Bolton [27]. It was ascribed to the participation of hot charge carriers in photodegradation processes. However, this phenomenon can be accounted for by considering the decrease of light absorption coefficient and partial escape of light from the reaction vial at long wavelengths. The photocatalytic activity of thin films (50–100 nm) of titania was reported to increase with the decrease of excitation light wavelength [29]. This is in agreement with the increase of light absorption coefficient for shorter wavelengths.

Fig. 5 shows the dependence of the pseudo-heterogeneous rate constant, defined by Eq. (17), of 2,4-D photodegradation with P-25 suspension on light intensity. The slope, 0.55 ± 10% in ln–ln coordinates indicates square root dependence of degradation rate on light intensity. The square root dependence of photodegradation rate on light intensity was observed in many works [30–33], however, linear dependence on light intensity is also often reported [34,35].

The experimental results of Fig. 4 were used to determine the effective value of photon capture cross-section by fitting results of Fig. 4 to Eq. (18), which is a general form of Eq. (7), Eqs. (14) and (15):

$$K^{1}_{ps}=K^{*}(1-\exp(-BG)) \qquad (18)$$

where G is the loading of titania in mg per cm^2 of vial cross-section area, K^* is the degradation rate coefficient at infinite loading of titania, and B is the coefficient related to average aggregate size. For P-25 TiO_2 the best fit was observed at values $K_{P\text{-}25}{}^{*}=0.096\pm0.004$; $B_{P\text{-}25}=5.6\pm0.9$. For Aldrich TiO_2 best fit was observed with $K_{Ald}{}^{*}=0.039\pm0.002$;

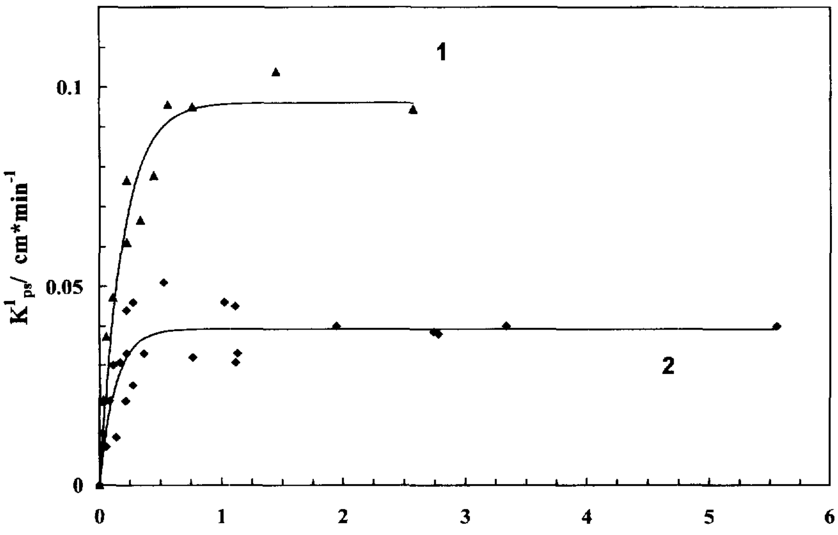

Fig. 4. Dependence of 2,4-D pseudo-heterogeneous photodegradation rate constant on loading of TiO_2 per unit area of illuminated vial cross-section; vial cross-section area 18 cm^2, solution volume 100 ml. Curve '1'- TiO_2 P-25,, curve '2'- TiO_2 Aldrich.

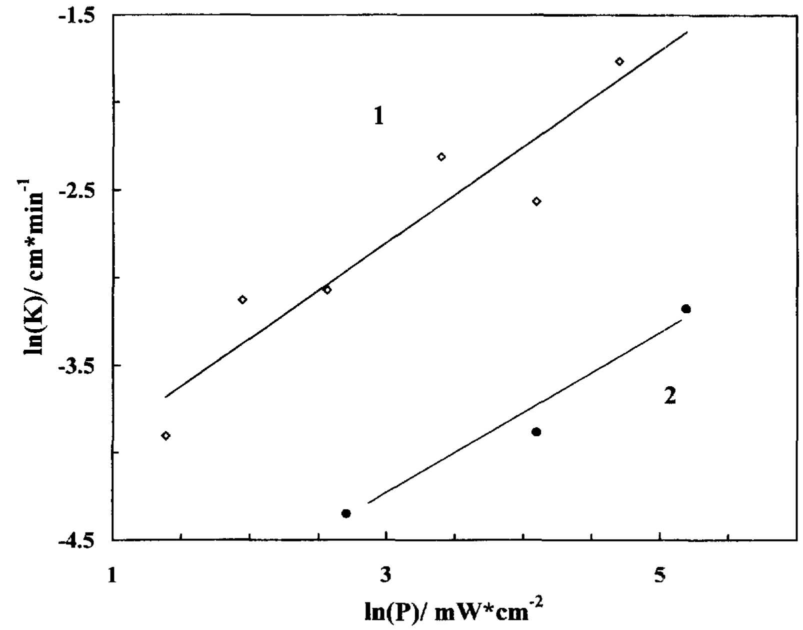

Fig. 5. Dependence of 2,4-D photodegradation rate constant on irradiation light. '1'-pseudo-heterogeneous rate constant in suspension of P-25, loading 0.22 mg per cm^2 of illuminated vial cross-section area; '2'-rate constant related per unit area of TiO_2 coated glass slide (P-25:Ormosil = 6).

$B_{\mathrm{Ald}} = 7.7 \pm 1.7$ The smooth curves of Fig. 3 were drawn using Eq. (18) with the relevant parameters. Taking into account that amount of the aggregates per cm^2 of vial surface area, nH are roughly equal to $nH = G10^{-3}/(D^3\rho)$, and taking photon capture cross-section as $\sigma = D^2$, where density of TiO_2 $\rho = 3.9$ g/cm, a rough estimate by Eq. (15) gives aggregate diameters of 480 nm and 330 nm, for P-25 and Aldrich TiO_2, respectively.

Eq. (15) is valid for $\alpha D \gg 1$. The value of α can be attributed to the average wavelength of irradiation used for excitation, $\lambda \approx 0.5\ (300+400) = 350$ nm. Using $\alpha = 1.4 \times 10^5$ cm^{-1} for $\lambda = 350$ nm, as given in [36], the product of αD for aggregates of TiO_2 P-25 and Aldrich is equal to 6.7 and 4.6, respectively. It indicates that nearly all light falling onto an aggregate of either titania P-25 or Aldrich is absorbed and supports the use of Eq. (15).

The above estimates of aggregate size were verified by measurements of particle size distribution conducted by light scattering measurements. For these measurements, sonicated suspensions of P-25 and Aldrich TiO_2 in 0.01 N $Na_2B_4O_7$ were prepared. A light beam of wavelength 632 nm was used. Photon energy of this light is far below the band gap of TiO_2

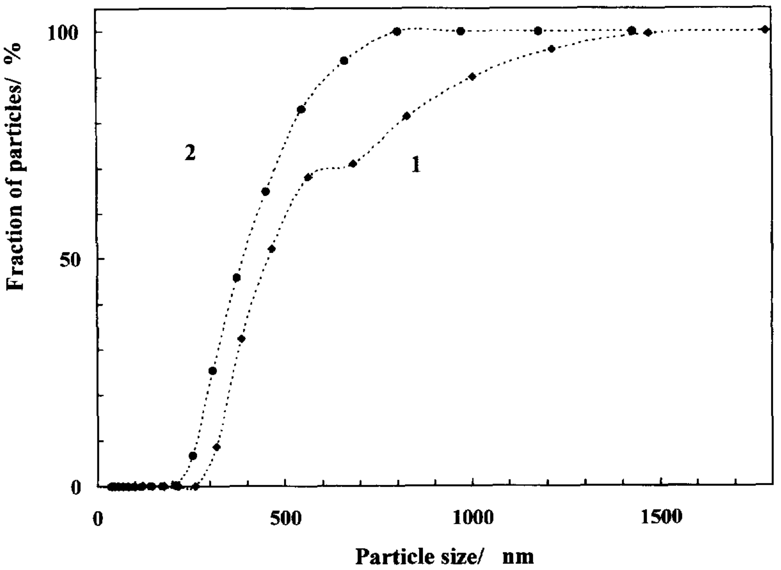

Fig. 6. Cumulative size distribution of aggregates in suspensions of TiO_2 P-25-'1' and TiO_2 Aldrich-'2' at pH 9.2.

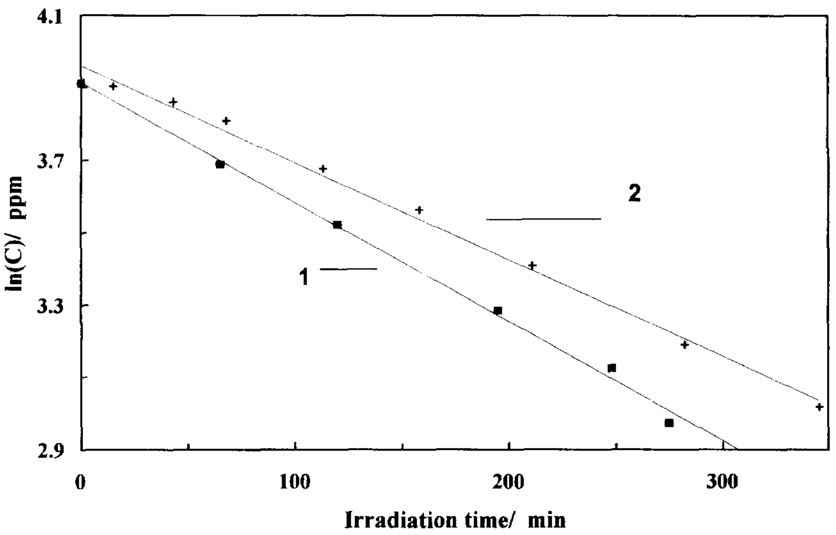

Fig. 7. Dependencies of logarithm of concentration of 2,4-D on time of irradiation of supported TiO_2 P-25 photocatalysts, initial concentration of 2,4-D 50 ppm. '1'-TiO_2 coated glass slide surface area 9.2 cm^2, solution volume 60 ml; '2'-0.3 g of floating catalyst (P-25:Eg:Ormosil = 1:1:1) solution volume 100 ml.

and more than 90% of the light flux was diffusely reflected. Cumulative particle size distribution curves are shown in Fig. 6. One can see relatively wide distribution of particle sizes in both cases. For Aldrich and P-25 TiO_2 80% of particles size distribution falls in the range of 270–620 nm and 320–1000 nm with mean average values of 320 nm and 418 nm, respectively. These values of the average particle size in suspensions are close to the values determined from the dependence of activity in suspension on the loading of TiO_2, Fig. 4, which supports the theoretical approach.

The curve of degradation of 2,4-D on thin P-25 film (P-25:Ormosil = 6) is shown in Fig. 7. Loading of TiO_2-Ormosil composition of 1.1 mg cm^{-2} corresponds to 2.4 micrometer of dense TiO_2. The value of the product (0.5 αh) = 17, which is much larger than 1. It enables one to consider the film of the catalyst as infinitely thick and to compare the measured degradation rate with the rate determined with P-25 suspension at infinite loading, $K_{P\text{-}25}$*. The value 2,4-D degradation rate coefficient normalised per illuminated surface of the plate S was $K_{pl}^* = (V/S)\mathrm{d}\{\ln C\}/\mathrm{d}t = 0.02$ cm min^{-1}. This value ($K_{P\text{-}25}^*/K_{pl}^* = 0.096/0.02$) is 5 times lower than the maximum value of 2,4-D pseudo-heterogenious degradation rate constant on P-25 suspension, under the same experimental conditions. However, Eqs. (7) and (15) account only for a twofold difference. The relatively low activity of supported P-25 can be ascribed to partial blocking of TiO_2 particles by the Ormosil binder.

Dependence of photodegradation rate constant measured with the thin TiO_2 film on light intensity is shown in Fig. 5. A square root dependence of 2,4-D degradation rate on light intensity was observed for suspension as well.

Curve '2' in Fig. 7 shows the degradation of 2,4-D using floating catalysts. Degradation rate observed in this case is related to the overall area occupied by the floating catalyst at the vial surface. The rate constant is 0.15 cm min^{-1}, which is 75% of the activity of the glass supported P-25 film. The difference in activity of the two forms of supported TiO_2 can be ascribed partially to gaps between floating particles and subsequent loss of light. The different P-25:Ormosil ratio and the presence of a third highly porous component—exfoliated graphite—could also influence the observed activity of the catalyst.

5. Conclusions

A simplified model of light distribution inside a vial filled with suspension of strongly absorbing light particles is proposed. The model was applied to describe the dependence of 2,4-D photodegradation on the concentration of suspension of P-25 and Aldrich TiO_2. The aggregate size obtained by modelling photodegradation process and by light scattering method was compared and gave a very good fit, which points on the reliability of the proposed approach.

Comparison of activity of suspended and supported photocatalyst based on the model presented here gives twice higher activity for the suspension (per unit illuminated area) as compared to the supported photocatalyst, provided that the excess photocatalyst loading is used in both cases, assuming lack of diffusion limitations and square root dependence of photodegradation on light intensity. However, the measured activity of TiO_2 on glass slide was approximately 5 times lower than activity of suspended TiO_2. The larger difference was ascribed to partial blocking of TiO_2 particles by the Ormosil binder.

Square root dependence of the photocatalytic activity on irradiation intensity was observed for TiO_2 P-25 in suspension and for TiO_2 P-25 supported on glass slide or floating particles of exfoliated graphite.

The activity of floating catalyst (P-25:Ormosil:Exfoliated Graphite = 1:1:1) per unit of vial cross-section area covered by floating particles was 75% of the activity TiO_2 film supported on glass slide.

Activity of TiO_2 P-25 suspension was approximately 2.5 times higher than that of Aldrich suspension. However, the Aldrich suspension formed smaller aggregates with narrower size distribution as compared to P-25 TiO_2.

6. List of symbols

$[AH_2]$	concentration of target compound in solution, mole cm^{-3}
C	concentration of 2,4-D in solution, mole cm^{-3} or ppm
d	diameter of photocatalyst particle, cm
D	aggregate size, cm
H	solution height in reaction vessel, cm
h	thickness of photocatalyst layer on support, cm
I	photon flux expressed as mole cm^{-2} s^{-1}
I_0	light flux hitting the solution or the upper layer of photocatalyst, mole cm^{-2} s^{-1}
k_{ox}	heterogeneous rate constant, $mole^{-1}$ cm^4 s^{-1}
K_{ps}	pseudo-heterogeneous rate constant, cm^2 $(s\ mole)^{-0.5}$
$K_{ps}{}^1 = K_{ps}\sqrt{I}$	the proportionality constant, cm s^{-1}
$K^* - K_{ps}{}^1$	for infinite loading of photocatalyst
K	the parameter characterising the photocatalytical properties of a single particle of photocatalyst
n	concentration of particles in suspension, cm^{-3}
$[p_s]$	surface concentration of holes, mole cm^{-3}
R	reflectivity coefficient
r	the rate of AH_2 oxidation by sngle particle of photocatalyst, mole s^{-1}
S	illuminated cross-section area of reaction vessel or photocatalyst film, cm^2
s	surface of a photocatalyst particle, cm^2
v	volume of a photocatalyst particle, cm^3
V	volume of reaction vessel, cm^3
w	photodegradation rate for supported photocatalyst, mole s^{-1}
x,y,z	coordinates
α	light absorption coefficient of photoctalyst, cm^{-1}
γ	form factor of photocatalyst particle
λ	irradiation wavelength, nm
$1-\theta$	void fraction of layer of photocatalyst
σ	photon capture cross-section of an aggregate, cm^2

Acknowledgements

We thank the BMBF, Germany and the Ministry of Science, Israel for supporting this research. The authors wish to express their gratitude to Dr. J. Gun and Dr. S. Sampath valuable remarks made during the preparation of the manuscript.

References

[1] E. Pramauro, E. Pelizzetti, Chemosphere 14 (1985) 195.
[2] M. Barbeni, M. Morello, E. Pramauro, E. Pelizzetti, M. Vincetti, E. Borgarello, N. Serpone, Chemosphere 16 (1987) 1165.

[3] A.L. Pruden, D.F. Ollis, Environ. Sci. Technol. 17 (1983) 628.
[4] A.L. Pruden, D.F. Ollis, J. Catal. 82 (1983) 404.
[5] R.W. Matthews, Water Research 20 (1986) 569.
[6] H. Al-Ekabi, N. Serpone, E. Pelizzetti, C. Minero, M.A. Fox, B. Draper, Langmuir 5 (1989) 250.
[7] N. Serpone, A. Bogarello, R. Harris, P. Cahill, M. Bogarello, Solar Energy Mater. 14 (1986) 121.
[8] A. Heller, M. Nair, L. Davidson, Z. Luo, J. Schwitzgebel, J. Norrel, J.B. Rock, S.-E. Lindquist, J.G. Ekerdt, in: D.F. Ollis, H. Al-Ekabi (Eds.), Photocatalytic Purification of Water and Air, Elsevier, New York, 1993, p. 139.
[9] M. Murabayashi, K. Itih, K. Kawashima, R. Masuda, S. Suzuki, in: D.F. Ollis, H. Al-Ekabi (Eds.), Photocatalytic Purification of Water and Air, Elsevier, New York, 1993, p. 783.
[10] R.W. Matthews, S.R. McEvoy, J. Photochem. Photobiol. A: Chem. 66 (1992) 355.
[11] R.W. Matthews, in: D.F. Ollis, H. Al-Ekabi (Eds.), Photocatalytic Purification of Water and Air, Elsevier, New York, 1993, p. 121.
[12] H. Gerischer, A. Heller, J. Electrochem. Soc. 139 (1992) 113.
[13] H. Gerischer, in: D.F. Ollis, H. Al-Ekabi (Eds.), Photocatalytic Purification of Water and Air, Elsevier, New York, 1993, p. 1.
[14] H. Gerischer, Electrochim. Acta 40 (1995) 1277.
[15] H.C. van de Hulst, Light Scattering by Small Particles, Wiley, New York, 1957, p. 470.
[16] M. Kerker, The scattering of light and other electromagnetic radiation, Academic Press, New York, 1969, p. 666.
[17] W.Wm. Wendlandt, H.G. Hecht, Reflectance spectroscopy, Interscience Publishers, Wiley, 1966, p. 300.
[18] P. Kubelka, J. Optical Soc. Amer. 38 (1948) 448.
[19] P.L. Yue, in: D.F. Ollis, H. Al-Ekabi (Eds.), Photocatalytic Purification of Water and Air, Elsevier, New York, 1993, p. 495.
[20] H. Al-Ekabi, N. Serpone, E. Pelizzetti, C. Minero, M.A. Fox, B. Draper, Langmuir 5 (1989) 250.
[21] M. Nargiello, T. Herz, in: D.F. Ollis, H. Al-Ekabi (Eds.), Photocatalytic Purification of Water and Air, Elsevier, New York, 1993, p. 801.
[22] L. Kavan, M. Grattzel, J. Rathousky, A. Zukal, J. Electrochem. Soc. 143 (1996) 394.
[23] A. Modestov, V. Glezer, I. Marjasin, O. Lev, J. Phys. Chem. B 101 (1997) 4623.
[24] M. Born, E. Wolf, Principles of Optics, Electromagnetic theory of propogation, interference, and diffraction of light, 5th edn., Pergamon, Oxford, 1975.
[25] P. Pichat, J.-C. D'Oliveira, J.-F. Maffre, D. Mas, in: D.F. Ollis, H. Al-Ekabi (Eds.), Photocatalytic Purification of Water and Air, Elsevier, New York, 1993, p. 683.
[26] J.F. Kenneke, J.L. Ferry, W. Glaze, in: D.F. Ollis, H. Al-Ekabi (Eds.), Photocatalytic Purification of Water and Air, Elsevier, New York, 1993, p. 179.
[27] J.E. Valladares, J.R. Bolton, in: D.F. Ollis, H. Al-Ekabi (Eds.) Photocatalytic Purification of Water and Air, Elsevier, New York, 1993, p. 111.
[28] H. Kawaguchi, in: D.F. Ollis, H. Al-Ekabi (Eds.), Photocatalytic Purification of Water and Air, Elsevier, New York, 1993, p. 665.
[29] T. Watanabe, A. Kitamura, E. Kojima, C. Nakayama, K. Hashimoto, A. Fujishima, in: D.F. Ollis, H. Al-Ekabi (Eds.), Photocatalytic Purification of Water and Air, Elsevier, New York, 1993, p. 747.
[30] K. Okamoto, Y. Yamamoto, H. Tanaka, A. Itaya, Bull. Chem. Soc. Jpn. 58 (1985) 2023.
[31] H. Al-Ekabi, N. Serpone, in: N. Serpone, E. Pelizzetti (Eds.), Photocatlysis. Fundumentals and applications, Wiley, New York, 1989, p. 457.
[32] G. Al-Sayyad, J.C. D'Oliveira, P. Pichat, J. Photochem. Photobiol. A 58 (1991) 99.
[33] T.P.M. Koster, J.W. Assink, J.M. Slaager, C. van der Veen, in: D.F. Ollis, H. Al-Ekabi (Eds.), Photocatalytic Purification of Water and Air, Elsevier, New York, 1993, p. 613.
[34] D.W. Bahnemann, D. Bocklemann, R. Goslich, M. Hilgendorf, D. Weichgrebe, in: D.F. Ollis, H. Al-Ekabi (Eds.), Photocatalytic Purification of Water and Air, Elsevier, New York, 1993, p. 301.
[35] J.B. Galves, S.M. Rodrigues, in: D.F. Ollis, H. Al-Ekabi (Eds.), Photocatalytic Purification of Water and Air, Elsevier, New York, 1993, p. 639.
[36] D.M. Eagles, J. Phys. Chem. Solids 25 (1964) 1243.